

Grey-Matter Atrophy in Alzheimer's Disease is Asymmetric but not Lateralized

Sabine Derflinger^{a,1}, Christian Sorg^{b,1}, Christian Gaser^c, Nicholas Myers^{d,e}, Milan Arsic^a, Alexander Kurz^b, Claus Zimmer^d, Afra Wohlschläger^{a,d} and Mark Mühlau^{a,*}

^aDepartment of Neurology, Technische Universität München, Munich, Germany

^bDepartment of Psychiatry, Technische Universität München, Munich, Germany

^cDepartment of Psychiatry, University of Jena, Jena, Germany

^dDepartment of Neuroradiology, Technische Universität München, Munich, Germany

^eGraduate School of Systemic Neuroscience, Ludwig-Maximilians-Universität München, Martinsried, Germany

Accepted 16 February 2011

Abstract. In Alzheimer's disease (AD), brain atrophy has been proposed to be left lateralized. Here, we reinvestigated the asymmetry and lateralization (i.e., asymmetry directed toward one hemisphere) of grey-matter (GM) distribution in 35 patients with AD, 24 patients with amnesic mild cognitive impairment (aMCI, a state of increased risk for AD), and 30 age-matched healthy controls (HC). We analyzed GM distribution by applying voxel-based morphometry (VBM) including analyses for asymmetry and lateralization. When comparing MCI with AD patients, VBM revealed GM loss in the entorhinal, temporoparietal, dorsofrontal, and occipital cortices as well as in the precuneus; when comparing HCs with MCI patients, we found similar differences, which were less pronounced especially within the temporoparietal cortex and precuneus. Analyses of regional asymmetry and regional lateralization as well as global lateralization did not yield significant results. However, lobar asymmetry of the temporal, parietal, and occipital lobes increased from HC to AD. Moreover, in aMCI and AD patients, performance of language-based neuropsychological tests correlated with lateralization of GM loss to the left hemisphere. We conclude that, in principle, brain atrophy in AD is asymmetric rather than lateralized. At the individual level however, asymmetry contributes to cognitive deficits.

Keywords: Alzheimer's disease, asymmetry, CERAD, lateralization, voxel-based morphometry

INTRODUCTION

In recent years, substantial progress has been made in understanding the pathophysiology of Alzheimer's disease (AD) [1]. Yet the mechanisms that ultimately give rise to its clinical picture are poorly understood. Consequently, discrimination of the spatial distribution of grey-matter (GM) loss is commonly regarded as a relevant contribution to this aspect of AD. Of particular interest are differences in GM loss between corresponding regions of both hemispheres, i.e., asym-

metry of brain atrophy, since its demonstration implies an interaction with factors involved in brain asymmetry [2, 3]. In accordance with the previous literature, we will refer to differences in GM between corresponding regions of the 2 hemispheres that are not necessarily directed towards one side as *asymmetry*. In contrast, asymmetry directed towards one hemisphere will be referred to as *lateralization*. Accordingly, asymmetry and lateralization are always the same at the individual level and can only diverge at the group level.

Brain asymmetry and lateralization have been observed in animals and humans at the structural, functional, and behavioral level with hereditary, environmental, and even pathological influences [4]. Besides handedness, specialization of the left hemisphere for language constitutes the earliest and

¹ These authors contributed equally to this work.

*Correspondence to: PD Dr. med. Mark Mühlau, Department of Neurology, Technische Universität München, Ismaningerstr. 22, D-81675 Munich, Germany. Tel.: +49 89 4140 4606; Fax: +49 89 4140 4867; E-mail: muehlau@lrz.tum.de.

most robust observation of functional lateralization. Correspondingly, the most striking structural brain asymmetry is observed around the perisylvian area with the planum temporale, the center of Wernicke's area, being much larger on the left [5]. Notably, some neurodegenerative diseases progress asymmetrically [4]. For example, motor symptoms of idiopathic Parkinson's disease are typically asymmetric with a trend towards the dominant hand [6]. In contrast, primary progressive aphasia typically shows left-lateralized brain atrophy in the perisylvian cortex as reflected by the common word-finding difficulties at onset [7]. In AD, however, data on asymmetry of atrophy are less clear.

Although possibly of low reliability [8], behavioral studies demonstrated an abnormal increase in functional asymmetry in AD patients [9, 10]. Others found a significant predominance of left-sided impairment [11] and even an influence of handedness [12]. Similarly, most studies using conventional nuclear medicine imaging techniques found metabolic brain asymmetry but no lateralization [13–20] but data on leftward lateralization also exist [21, 22]. Likewise, magnetic resonance imaging (MRI) data yielded left-lateralized atrophy of several cortical areas [23–26] but not of the hippocampus [27]. Histopathological studies demonstrated asymmetric but not lateralized distribution of neurofibrillary tangles and plaques [28–30]. Recent positron emission tomography (PET) studies of plaques *in vivo*, and hence in earlier stages, indicated leftward lateralization within the dorsal frontal cortex and sensory-motor area in mild cognitive impairment (MCI) and AD patients, while most areas displayed symmetric plaque load [31]. Evidence for asymmetric effects in animal models is even more sparse [32].

Of note, most studies that reported asymmetry or lateralization in AD referred merely to visual impressions. If statistical tests were performed, the number of patients was small. Therefore, we investigated asymmetry of brain atrophy in AD by statistical means in a relatively large cohort of patients representing different stages of the disorder, ranging from a state of high risk for AD, amnesic MCI (aMCI), to later stages. Moreover, we related our findings to neuropsychological data.

METHODS

Subjects

The study was performed in accord with the Helsinki Declaration of 1975. Beforehand, we obtained written informed consent from each participant and approval by the local ethics committee. We recruited 35 patients with AD and 24 with aMCI from our Memory Clinic (Technische Universität München, Munich, Germany). Thirty healthy controls (HC) were recruited by word-of-mouth advertising and only included in case of unremarkable neuropsychiatric evaluation. Demographic and neuropsychological data of the participants are given in Table 1. All patients underwent psychiatric evaluation, neurological examination, standard laboratory testing, and neuropsychological testing including the Clinical Dementia Rating (CDR) and CERAD ("Consortium to Establish a Registry for AD") protocol.

The criteria for aMCI were the following [33, 34]: memory complaints of the patient objectified by at least one pathological subtest in the CERAD test battery (Z value ≤ 1.0) and, preferably supported by an infor-

Table 1
Demographical data and neuropsychological parameters

	HC	aMCI	AD	<i>p</i> value
<i>N</i>	30	24	35	n/a
Age (mean \pm sd)	67 \pm 8.7	69 \pm 9.0	71.1 \pm 8.7	n.s.
Female/male	20/10	13/11	16/19	n.s.
Right-handedness (%)	100	100	100	n.s.
CDR	n.d.	0.5 (24)	1 (23), 2 (12)	<0.001
MMSE (absolute values, 0–30)	n.d.	26.8 \pm 1.7	21.1 \pm 4.6	<0.001
CERAD data (<i>Z</i> value)				
MMSE	n.d.	-1.9 \pm 1.5	-6.8 \pm 4.4	<0.001
Verbal fluency	n.d.	-1.0 \pm 1.1	-1.8 \pm 1.0	<0.05
Boston naming test	n.d.	-0.14 \pm 1.5	-1.6 \pm 2.2	<0.05
Wordlist memory	n.d.	-1.7 \pm 1.2	-3.4 \pm 1.4	<0.001
Wordlist recall	n.d.	-1.9 \pm 1.2	-2.7 \pm 1.1	<0.05
Constructional praxis	n.d.	-0.87 \pm 1.7	-2.8 \pm 3.4	<0.05
Constr.prx. recall	n.d.	-1.2 \pm 1.2	-3.3 \pm 1.7	<0.001
Education (years)	10.6 \pm 1.7	10.4 \pm 2.0	9.9 \pm 2.5	n.s.

MMSE, mini-mental state examination; n/a, not applicable; n.d., not determined; n.s., not significant.

mant, preserved general cognitive function, intact activities of daily living, as well as no dementia according to the Clinical Dementia Rating (CDR = 0.5). The 24 aMCI patients were classified [35] as multiple-domain aMCI ($n = 22$), and single-domain aMCI ($n = 2$). All AD patients met the criteria of the National Institute of Neurological and Communicative Disorders and Stroke and Related disorders Task Force [36]. Scores of the CDR were 1 ($n = 23$) and 2 ($n = 12$) exclusively (mild to moderate AD). Forty-seven patients were excluded from the original cohort of 108 patients. Exclusion criteria were relevant neurological or psychiatric disease (e.g., stroke, somatoform pain disorder, chronic alcohol abuse, restless legs syndrome, or head trauma), motion artifacts on MRI, no clear attribution to one group according to the above mentioned criteria, and left-handedness. Moreover, MRIs showing more than 2 white matter lesions over 10 mm or 8 lesions between 5 and 9 mm on FLAIR images were excluded as proposed by Bozzali et al. [37].

Magnetic resonance imaging

All brain images were acquired on the same 3 T scanner (Achieva, Philips, Netherlands). For voxel-based morphometry (VBM), we used a 3D gradient echo T1-weighted sequence (orientation, 170 contiguous sagittal 1 mm slices; field of view, 240×240 mm; in plane resolution, 240×240 mm; voxel size, $1.0 \times 1.0 \times 1.0$ mm; repetition time, 9 ms; echo time, 4 ms). To evaluate white matter lesions, we used FLAIR images (orientation, 36 contiguous axial 4 mm slices; field of view, 230×184 mm; in plane resolution, 240×138 mm; voxel size, $0.96 \times 1.33 \times 4.0$ mm; repetition/inversion time 11000/2800 ms; echo time, 120 ms). SPM8 software (Wellcome Department of Imaging Neuroscience Group, London, UK; <http://www.fil.ion.ucl.ac.uk/spm>) and the VBM8 toolbox (<http://dbm.neuro.uni-jena.de/vbm.html>) were applied for data processing.

Voxel-based morphometry

For VBM, images were corrected for bias-field inhomogeneities, registered using linear (12-parameter affine) and nonlinear transformations, and tissue-classified into GM, white matter (WM), and cerebrospinal fluid (CSF) within the same generative model [38]. The segmentation procedure was further refined by accounting for partial volume effects [39], by applying adaptive maximum a posteriori estima-

tions [40], and by applying a hidden Markov random field model [41] as proposed recently [42]. We used a template which was rendered symmetric around the midsagittal plane to enable later voxel-based asymmetry analysis. The resulting GM images were modulated to account for volume changes resulting from the normalization process. Here, we considered only non-linear volume changes so that further analyses did not have to account for differences in head size. Finally images were smoothed with a Gaussian kernel of 8 mm (FWHM).

Global values of GM, WM, and CSF were derived from the first segmentation process. These values were corrected for head size through division by the total intracranial volume (TIV), which was approximated by the sum of global GM, WM, and CSF.

Voxel-wise analysis of asymmetry and lateralization

As described above, we refer to differences in GM between corresponding regions of the 2 hemispheres that are not necessarily directed towards one side as brain asymmetry while asymmetry directed towards one hemisphere is referred to as lateralization. For voxel-wise analysis of asymmetry (VBMasym) and lateralization (VBMlat), we used an extension of VBM which has been validated and described by Lüders [43]. Accordingly, we generated one difference image (DI) of each participant in an additional step before smoothing (FWHM, 8 mm). In essence, the voxels of these images comprise the relative (not absolute) surplus of GM in relation to the corresponding voxel of the other hemisphere. To this end, the original GM images (origGM) were flipped along the midsagittal plane (flipGM). Then, we calculated the lateralization index of each voxel by applying the following formula: $(\text{origGM} - \text{flipGM}) / (0.5(\text{origGM} + \text{flipGM}))$ or, with other words, the differences between both images were divided by the mean of both images in a voxel-wise manner. This procedure resulted in DIs in that the corresponding voxels of both hemispheres contain numbers with the same numerical part but the opposite sign (i.e., plus and minus).

To compare asymmetry and lateralization among groups, we used the DIs for the following analyses:

1. Regional asymmetry (VBMasym): to detect regions of significantly increased asymmetry, we generated variance-focused F-maps (as implemented in SPM8) through voxel-wise comparison of the smoothed DIs by creating an

ANOVA model including all 3 groups and *T*-tests for pair-wise group comparisons.

2. Regional lateralization (VBMIlat): to detect regions of significant lateralization, we generated mean-focused T-maps (as implemented in SPM8) through voxel-wise comparison of the smoothed DIs by creating an ANOVA model including all 3 groups and *T*-tests for pair-wise group comparisons.
3. Global measures of asymmetry and lateralization: we calculated global measures of asymmetry and lateralization with regard to the hemispheres and brain lobes. Therefore, the voxel values (VBM) of each lobe and hemisphere as defined by the pickatlas [44] were summed up. Again, we calculated the lateralization index which was used for the analysis of lateralization whereas its numerical part was used for the analysis of asymmetry.

Statistical analysis

For group comparisons of parametric demographic and neuropsychological data as well as global imaging values, analysis of variance (ANOVA, including all 3 groups) and *T*-tests (pair-wise group comparisons) were performed. For group comparisons of gender, Fisher's exact test was applied (Software, SPSS statistics 18.0). Only 2-sided *P* values are given.

All voxel-wise comparisons (VBM, VBMIlat, and VBMIasym) were restricted to voxels with an *a-priori* GM probability of >0.1 in order to include only voxels with sufficient GM and to avoid borderline effects between GM and WM.

Of note, the definitions of asymmetry and lateralization imply that with regard to a certain brain region, asymmetry other than lateralization can only refer to the group level whereas lateralization can refer to both the individual and group level. Hence, analysis of asymmetry and lateralization is justified for group comparisons. However, correlation analyses of individual test performance can, again, only be meaningful with regard to lateralization since we expect individual test performance to correlate with GM loss directed towards one hemisphere (lateralization) rather than with GM loss directed towards one or the other hemisphere (asymmetry).

For group comparisons, the HC and aMCI group, the HC and AD group, as well as the aMCI and AD group were compared in a pair-wise manner (*T*- and *F*-tests extended by the nuisance variables of age, gender, and education in years).

In order to analyze the functional relevance of individual lateralization, voxel-wise correlation analyses with neuropsychological parameters were performed by the use of a simple regression model, which included all 61 patients (VBM and VBMIlat). The following neuropsychological parameters of the CERAD test battery were analyzed: Boston naming test, verbal fluency, word list recall, word list memory, constructional praxis, and recall of constructional praxis. These parameters were *z*-transformed to normalize for age, gender, and education so that we did not have to include these parameters as nuisance variables. We accounted for the possibility of different underlying causes of regional lateralization, namely GM loss within one hemisphere, GM preservation within the other hemisphere, or combination of both effects. To address this issue, we extracted the coordinates of each cluster peak derived from VBMIlat and then extracted the values of this voxel and its contralateral counterpart from the corresponding VBM. These values were then fed into a multiple regression model with the neuropsychological parameter as dependent and the 2 voxel values (left and right) as independent variables.

For statistical thresholding, we used a novel technique [45] called threshold-free cluster enhancement (TFCE). This method takes a raw statistic image and produces an output image in which the voxel-wise values represent the amount of cluster-like local spatial support over voxel threshold. Significance and its correction for multiple comparisons is then determined via permutation testing so that clusters are determined without arbitrary height thresholds (i.e. "threshold free") and even largely independent from spatial smoothing. We performed 1000 permutations and set the significance threshold to 0.05 corrected (family-wise error). For exploratory analyses, we relaxed the significance threshold to 0.001 uncorrected.

For localization of GM changes (peak voxels), we used the anatomy toolbox as implemented in SPM8 (http://www.fz-juelich.de/inm/inm-1/spm_anatomy_toolbox).

RESULTS

Demographic and neuropsychological data

The demographic and neuropsychological data are given in Table 1. As expected, scores of the mini-mental state examination (MMSE) were significantly lower in the AD group than in the aMCI group ($p < 0.001$). The AD group performed significantly

poorer in all other subtests of the CERAD protocol (Table 1).

Voxel-based morphometry – group comparisons

All group comparisons of global GM (GM/TIV) yielded significant results (T -tests, $p < 0.003$). The voxel-wise comparison of the aMCI and AD groups revealed GM loss in the entorhinal, temporoparietal, dorsofrontal, and occipital cortices as well as in the precuneus whilst comparison of the HC and aMCI groups yielded similar differences that were less pronounced especially within the temporoparietal cortex and precuneus (Fig. 1, Table 2). None of the tests of the VBMIlat and VBMIasym showed significant results even after exploratory lowering of the statistical thresh-

old. Likewise, global measures of lateralization did not differ significantly, nor did asymmetry of the frontal lobe. In contrast, the remaining 4 global measures of asymmetry (temporal, parietal, and occipital lobe as well as hemisphere) increased significantly from HC to AD (4 ANOVAs, each $p < 0.006$). Significant results of pair-wise group comparisons are shown in Fig. 2.

Voxel-based morphometry – neuropsychological parameters

Analyzing language-based tests (VBM) demonstrated correlation of word list memory with left-sided GM reaching from the precuneus across superior parietal and lateral posterior temporal areas to the planum temporale (Fig. 3, left upper panel; Table 3). VBMIlat

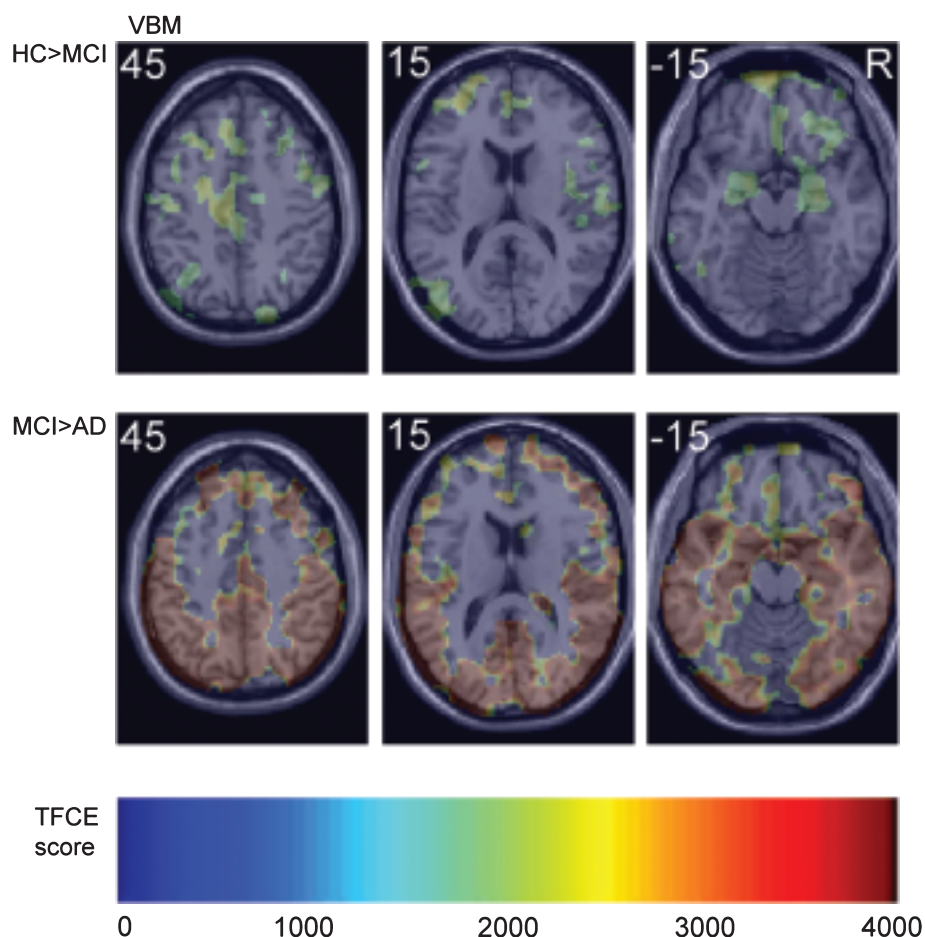


Fig. 1. Group comparisons of grey-matter loss derived from conventional VBM. Axial slices of GM loss are projected onto the SPM template. MNI coordinates are indicated in the left upper corners. The smoothed GM images were fed into T -tests. Healthy controls compared to aMCI patients are demonstrated in the upper row, aMCI compared to AD patients in the middle row. Statistical thresholds were calculated by the use of threshold-free cluster enhancement (TFCE). Only voxels surviving a significance threshold of $p < 0.05$ corrected are shown. Increasing significance according to the TFCE score is color-coded as indicated by the bar at the bottom. Color coding was limited to a TFCE score of 4000 for visibility.

Table 2
Group comparisons derived from voxel-based morphometry

MNI coordinates of peak voxels	Anatomical region	Cluster size	<i>p</i> -value corrected	<i>p</i> -value uncorrected	TFCE score
Healthy controls > patients with mild cognitive impairment (VBM)					
-26 -13 -12	Hippocampus L	1705	0.024	0.004	1991
-16 0 -17	Parahippocampal g. L		0.029	0.004	2098
-18 -5 -8	Amygdala L		0.045	0.005	2102
-27 -85 6	Middle occipital g. L	5787	0.028	0.004	2103
-10 -21 43	Middle cing. cortex L	43626	0.028	0.004	2382
28 56 -3	Sup. orbital g. R		0.049	0.006	2389
-26 54 7	Middle frontal g. L		0.048	0.005	2585
Patients with mild cognitive impairment > patients with Alzheimer's disease (VBM)					
0 -55 54	Precuneus L	332525	0.001	<0.001	9347
52 -64 42	Angular g. R		0.001	0.001	9296
58 -45 -21	Inferior temporal g. R		0.001	0.001	9214
32 -72 25	Middle occipital g. R		0.001	0.001	9137
-63 -55 12	Middle temporal g. L		0.001	0.001	9101
-24 -78 45	Sup. parietal lobule L		0.001	0.001	9083
-4 40 54	Sup. medial g. L		0.005	0.001	5215

Note: Anatomical regions were derived from the Anatomy toolbox as implemented in SPM8. Cing., cingulate; g., gyrus; L, left; MNI, Montreal Neurological Institute; R, right; sup., superior; TFCE, threshold-free cluster enhancement.

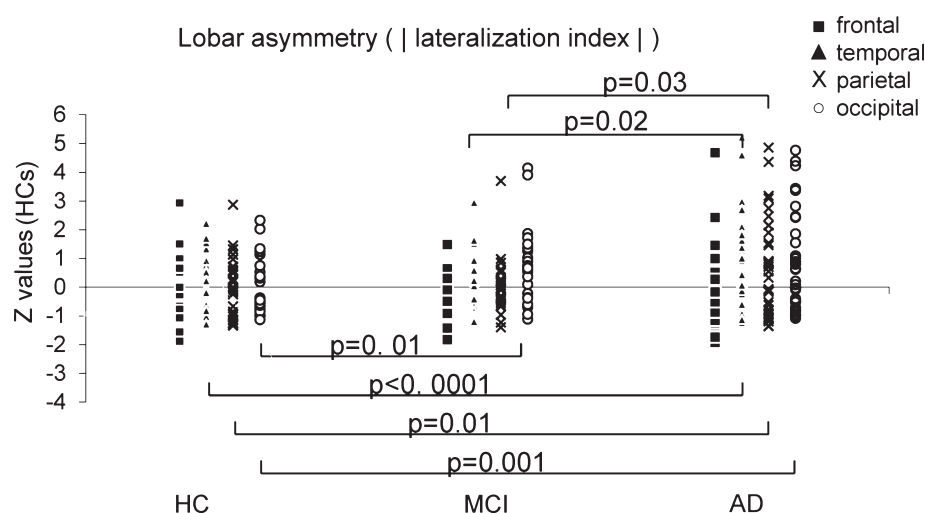


Fig. 2. Lobar asymmetry. Plots of lobar asymmetry values were *z* transformed according to the mean value and standard deviation of HC. Mean values of lobar asymmetry differed among groups apart from the frontal lobe. *p* values derived from pair-wise group comparisons are indicated. AD, Alzheimer's disease; HC, healthy controls; MCI, mild cognitive impairment.

confirmed left-lateralized GM loss within the planum temporale (Fig. 3, right upper panel; Table 3). A similar but less lateralized pattern of GM loss resulted from the correlation with recall of word list memory (VBM). Here, VBMat did not yield significant results even after exploratory analyses with more liberal thresholds (not shown). The remaining language-based tests, i.e., the Boston naming and verbal fluency test, showed pronounced perisylvian GM loss (VBM) predominantly on the left. Once more, this impression could not be confirmed by VBMat although after relaxing the statistical threshold, clusters appeared on the

left (not shown). In particular, the Boston naming test also revealed the left planum temporale while the verbal fluency test was related to leftward lateralization in the anterior insula and frontal operculum. Multiple regression analyses of left-hemispheric peak voxels (coordinates derived from VBMat including the exploratory findings) and their right counterpart (both values derived from VBM) demonstrated that all clusters of left-lateralized GM loss resulted exclusively from left-sided GM loss (voxel values of the left, $p < 0.01$ voxel values of the right, $p > 0.1$) although the left and right value were always strongly

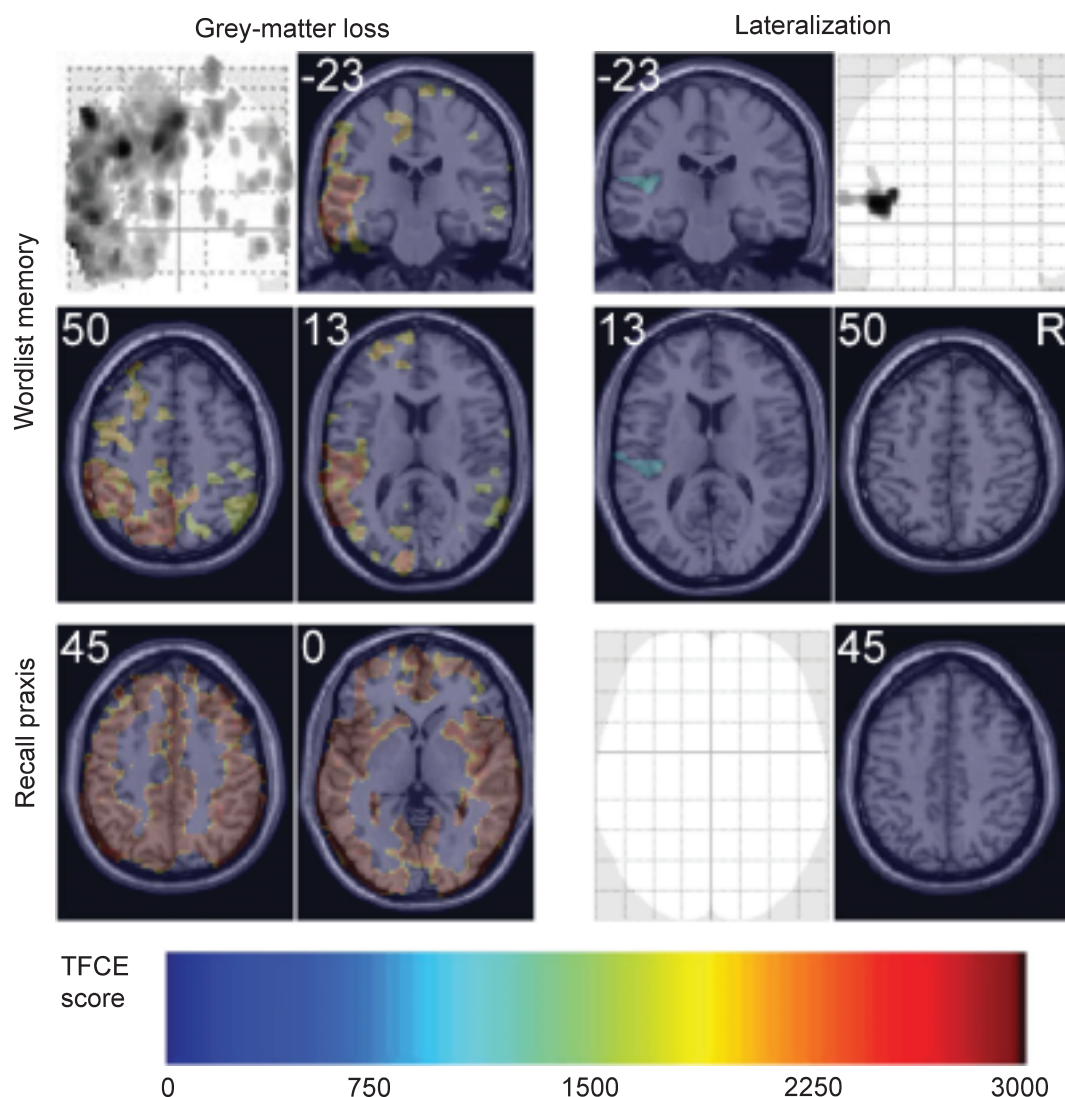


Fig. 3. Relation of regional grey-matter and its lateralization to neuropsychological performance. Analyses of regional GM are displayed in the left column and analysis of its lateralization in the right column (axial slices projected onto the SPM template and maximum intensity projections). MNI coordinates are indicated in the left upper corners. The smoothed GM and DI images were fed into regression analyses. Upper panel: correlation of word list memory performance with GM (left, VBM) yields left-lateralized GM loss pronounced in the planum temporale and precuneus; this visual impression was confirmed by lateralization analyses within the planum temporale (right; VBMIlat). Middle panel: correlation of recall of constructional praxis with GM yields wide-spread GM loss similar to that of the group comparison; lateralization analysis did not yield significant results as symbolized by the empty axial slice and maximum intensity projection. Statistical thresholds were calculated by the use of threshold-free cluster enhancement (TFCE). Only voxels surviving a significance threshold of $p < 0.05$ corrected are shown. Increasing significance according to the TFCE score is color-coded as indicated by the bar at the bottom. Color coding was limited to a TFCE score of 3000 for visibility.

correlated (Pearson's correlation coefficient >0.5 ; $p < 0.001$).

Analyzing constructive praxis-based tests demonstrated no significant correlation of GM loss with constructional praxis while its recall was associated with widespread bilateral GM loss (Fig. 3, left middle panel; Table 3) comprising the temporal, parietal and occipital cortex (VBM). No lateralization was found

(Fig. 3, right middle panel) even after relaxing the significance thresholds.

DISCUSSION

We investigated asymmetry and lateralization of brain atrophy in AD and aMCI, a state of high risk (approx. 50%/2 y) for conversion to AD [46], at the

Table 3
Correlation of regional grey-matter loss (VBM) and its lateralization (VBMLat) with neuropsychological performance

MNI coordinates of peak voxels	Anatomical region	Cluster size	<i>p</i> -value corrected	<i>p</i> -value uncorrected	TFCE score
Wordlist memory – lateralization (VBMLat)					
–45 –24 10	Sup. temporal g. L (planum temporale)	562	0.015	0.001	1071
Wordlist memory – grey matter (VBM)					
–66 –7 –9	Middle temporal g. L	116688	0.006	0.001	3257
–48 –51 39	Inf. parietal lobule L		0.009	0.002	3256
–14 –70 45	Sup. parietal lob. R		0.007	0.001	3296
–62 –39 –17	Inf. temporal g. L		0.006	0.001	3255
–6 –66 39	Precuneus L		0.007	0.001	3311
Constructional praxis recall – lateralization (VBMLat)					
–	–	–	–	–	–
Constructional praxis recall – grey matter (VBM)					
–57 –55 10	Middle temporal g. L	336045	0.002	<0.001	6460
57 –52 46	Inf. parietal lobule R		0.003	0.001	6454
–48 –49 27	Supramarginal g. L		0.003	0.001	6268
–14 –58 45	Precuneus L		0.003	0.001	6065
62 –33 4	Middle temporal g. R		0.003	0.001	6027

Note: Anatomical regions were derived from the Anatomy toolbox as implemented in SPM8. g., gyrus; inf., inferior; L, left; MNI, Montreal Neurological Institute; R, right; sup., superior; TFCE, threshold-free cluster enhancement.

regional and global level. We argue that, in principle, brain atrophy in AD is asymmetric rather than lateralized, that data suggesting leftward lateralization may have resulted from a selection bias, and that individual asymmetry (i.e., lateralization) seems to contribute to cognitive deficits.

With regard to group comparisons, our data are plausible and in line with previous findings. VBM yielded robust results in accordance with earlier reports [37, 47–51], but we could neither demonstrate asymmetry (VBM_{asym}) nor lateralization (VBMLat) at the group level. However, global measures of GM asymmetry derived from the temporal, parietal, and occipital (but not frontal) lobe as well as the whole hemisphere increased from HC to AD indicating that AD pathology tends to affect brain lobes and even the hemispheres to different extents in an asymmetric but not lateralized manner. Asymmetry of occipital lobe atrophy may seem surprising but has also been reported by others [24]. Our findings are compatible with several conventional nuclear imaging studies that showed asymmetry but no lateralization while operating at lower spatial resolution and, hence, between the spatial levels of voxel size and brain lobe [13–20]. Most similar to our approach, Kovalev et al. calculated lobar asymmetry values from SPECT data and found all lobes to be more asymmetric (but, again, not lateralized) in AD than in HC [16].

However, there are also substantial data pointing to a leftward lateralization of atrophy in AD while we are only aware of one report suggesting rightward lateralization [52]. Some of the studies indicating

lateralization did not compare the 2 hemispheres by statistical means. Assuming asymmetry, it seems possible that, dependent on the statistical threshold chosen, statistical parametric maps generated the visual impression of lateralization although this impression would not have survived statistical testing [23, 25, 49, 52]. Still, Thompson and colleagues [24] used an image analysis technique known as cortical pattern matching in 12 AD patients and, by statistical means, demonstrated leftward lateralization of regional GM loss and its increase over the mean follow-up interval of 2.1 years. Yet the observation of longitudinal increase of leftward atrophy *per se* does not further support the assumption of left-lateralized brain atrophy which is a special form of asymmetry and both of these possibilities are almost certain to develop over time and, hence, to further increase once they exist. Accordingly, asymmetric brain metabolism in AD has also been demonstrated to increase over time [15]. Furthermore, the chance selection of a small sample of patients with left-lateralized atrophy from a population with asymmetric atrophy (i.e., a mixture of right and left lateralized atrophy!) is well conceivable while the opposite, the selection of a sample with asymmetric brain atrophy from a population with (only!) left-lateralized brain atrophy, is not. This possibility would imply a selection bias which may have arisen from the fact that clinical scores are primarily language-based resulting in a bias towards selection of patients with left-lateralized atrophy. This explanation has already been suggested by others [19] and complies with our finding of a significant correlation

between language-based tests and left-lateralized brain atrophy.

In line with basic concepts of language processing [53], tasks requiring language production correlated primarily with left anterior regions and performance requiring language perception primarily with left posterior regions. Yet, lateralization according to the predefined significance thresholds could only be demonstrated for word list memory within the left planum temporale. Involvement of this region in phonological working memory has been postulated [54] and was recently demonstrated for auditory short-term memory of digits which resembles the word list memory task of the CERAD protocol [55]. Of note, correlation with test performance was much stronger for regional GM loss than for its lateralization as demonstrated by the large differences of the respective TFCE scores (Fig. 3). The fact that only left-sided GM loss explained variance in test performance points in the same direction as do results derived from surface-based MRI morphometry [56]. Insofar, we could demonstrate lateralization only for the most lateralized tasks (i.e., testing of language-based skills) within the most asymmetric brain region, namely the planum temporale [4]. Only under this condition, the regional GM of one side correlated so strongly with test performance (VBM) that it remained significant after including additional variance from the inefficient right hemisphere (VBMlat). Lending support to this idea, our explanatory analyses yielded further correlations of left-lateralized GM loss for tests requiring language production within the second-most asymmetric brain region, the anterior perisylvian area. The finding of functionally relevant regional leftward lateralization has also been demonstrated by others for brain metabolism [57]. Yet in the light of overall asymmetry, these findings raise the question of functionally relevant rightward lateralization which was, indeed, demonstrated in several PET studies in which tests other than the CERAD protocol were applied. Meguro et al. investigated 34 AD patients of whom 14 had a leftward and 12 had a rightward impairment of visuospatial attention. This asymmetrically impaired function corresponded to a contralateral decrease in absolute regional cerebral blood flow within the parietal lobe [17]. Moreover, Haxby et al. reported asymmetry of regional cerebral metabolic rate of glucose to correspond with asymmetry of language and visuospatial functions [14]. Likewise, functionally relevant asymmetry of glucose metabolism was found to correlate with semantic and non-semantic memory capacity [21]. In conclusion, accumulating evidence

from PET data also lend support to the notion of functionally relevant hemispheric asymmetry in AD.

Our study has some limitations. Apart from the educational level, neuropsychological performance of our HCs was not examined. No neuropsychological tests representing right hemispheric function were performed so that the demonstration of functionally relevant asymmetry remains incomplete. Moreover, our aMCI group is unlikely to completely represent the precursor of AD [46]. Finally, we cannot draw conclusions about the dynamics of asymmetry in AD from our cross-sectional design.

In summary, our data demonstrate that, in principle, brain atrophy in AD is asymmetric rather than lateralized. At the individual level, however, asymmetry seems to contribute to cognitive deficits to a certain degree.

ACKNOWLEDGMENTS

We thank Markus Ploner for very helpful comments on an earlier version of the manuscript.

This work was supported by KKF (Kommission für Klinische Forschung des Klinikums rechts der Isar der Technischen Universität München) Grant B08-09 to Derflinger S, by KKF Grant 8765160 to Sorg C, by Merck Serono to Arsic M, and by German Federal Ministry of Education and Research Grant 01EV0710 to Wohlschläger A.

Authors' disclosures available online (<http://www.j-alz.com/disclosures/view.php?id=777>).

REFERENCES

- [1] Querfurth HW, LaFerla FM (2010) Alzheimer's disease. *N Engl J Med* **362**, 329-344.
- [2] Hutsler J, Galuske RA (2003) Hemispheric asymmetries in cerebral cortical networks. *Trends Neurosci* **26**, 429-435.
- [3] Kristofikova Z, Kozmikova I, Hovorkova P, Ricny J, Zach P, Majer E, Klaschka J, Ripova D (2008) Lateralization of hippocampal nitric oxide mediator system in people with Alzheimer disease, multi-infarct dementia and schizophrenia. *Neurochem Int* **53**, 118-125.
- [4] Toga AW, Thompson PM (2003) Mapping brain asymmetry. *Nat Rev Neurosci* **4**, 37-48.
- [5] Steinmetz H (1996) Structure, functional and cerebral asymmetry: *in vivo* morphometry of the planum temporale. *Neurosci Biobehav Rev* **20**, 587-591.
- [6] Uitti RJ, Baba Y, Whaley NR, Wszolek ZK, Putzke JD (2005) Parkinson disease: handedness predicts asymmetry. *Neurology* **64**, 1925-1930.
- [7] Mesulam MM (2003) Primary progressive aphasia – a language-based dementia. *N Engl J Med* **349**, 1535-1542.
- [8] Xeno Rasmusson D, Brandt J (1995) Instability of cognitive asymmetry in Alzheimer's disease. *J Clin Exp Neuropsychol* **17**, 449-458.

- [9] Massman PJ, Doody RS (1996) Hemispheric asymmetry in Alzheimer's disease is apparent in motor functioning. *J Clin Exp Neuropsychol* **18**, 110-121.
- [10] Strite D, Massman PJ, Cooke N, Doody RS (1997) Neuropsychological asymmetry in Alzheimer's disease: verbal versus visuoconstructional deficits across stages of dementia. *J Int Neuropsychol Soc* **3**, 420-427.
- [11] Capitani E, Della Sala S, Spinnler H (1990) Controversial neuropsychological issues in Alzheimer's disease: influence of onset-age and hemispheric asymmetry of impairment. *Cortex* **26**, 133-145.
- [12] Doody RS, Vacca JL, Massman PJ, Liao TY (1999) The influence of handedness on the clinical presentation and neuropsychology of Alzheimer disease. *Arch Neurol* **56**, 1133-1137.
- [13] Friedland RP, Budinger TF, Koss E, Ober BA (1985) Alzheimer's disease: anterior-posterior and lateral hemispheric alterations in cortical glucose utilization. *Neurosci Lett* **53**, 235-240.
- [14] Haxby JV, Duara R, Grady CL, Cutler NR, Rapoport SI (1985) Relations between neuropsychological and cerebral metabolic asymmetries in early Alzheimer's disease. *J Cereb Blood Flow Metab* **5**, 193-200.
- [15] Haxby JV, Grady CL, Koss E, Horwitz B, Heston L, Schapiro M, Friedland RP, Rapoport SI (1990) Longitudinal study of cerebral metabolic asymmetries and associated neuropsychological patterns in early dementia of the Alzheimer type. *Arch Neurol* **47**, 753-760.
- [16] Kovalev VA, Thurfjell L, Lundqvist R, Pagani M (2006) Asymmetry of SPECT perfusion image patterns as a diagnostic feature for Alzheimer's disease. *Med Image Comput Assist Interv* **9**, 421-428.
- [17] Meguro K, Shimada M, Someya K, Horikawa A, Yamadori A (2001) Hemispatial visual-searching impairment correlated with decreased contralateral parietal blood flow in Alzheimer disease. *Neuropsychiatry Neuropsychol Behav Neurol* **14**, 213-218.
- [18] Volkow ND, Zhu W, Felder CA, Mueller K, Welsh TF, Wang GJ, de Leon MJ (2002) Changes in brain functional homogeneity in subjects with Alzheimer's disease. *Psychiatry Res* **114**, 39-50.
- [19] Keilp JG, Alexander GE, Stern Y, Prohovnik I (1996) Inferior parietal perfusion, lateralization, and neuropsychological dysfunction in Alzheimer's disease. *Brain Cogn* **32**, 365-383.
- [20] Duara R, Grady C, Haxby J, Sundaram M, Cutler NR, Heston L, Moore A, Schlageter N, Larson S, Rapoport SI (1986) Positron emission tomography in Alzheimer's disease. *Neurology* **36**, 879-887.
- [21] Zahn R, Juengling F, Bubrowski P, Jost E, Dykierck P, Talazko J, Huehl M (2004) Hemispheric asymmetries of hypometabolism associated with semantic memory impairment in Alzheimer's disease: a study using positron emission tomography with fluorodeoxyglucose-F18. *Psychiatry Res* **132**, 159-172.
- [22] Loewenstein DA, Barker WW, Chang JY, Apicella A, Yoshii F, Kothari P, Levin B, Duara R (1989) Predominant left hemisphere metabolic dysfunction in dementia. *Arch Neurol* **46**, 146-152.
- [23] Janke AL, de Zubicaray G, Rose SE, Griffin M, Chalk JB, Galloway GJ (2001) 4D deformation modeling of cortical disease progression in Alzheimer's dementia. *Magn Reson Med* **46**, 661-666.
- [24] Thompson PM, Hayashi KM, de Zubicaray G, Janke AL, Rose SE, Semple J, Herman D, Hong MS, Dittmer SS, Doddrell DM, Toga AW (2003) Dynamics of gray matter loss in Alzheimer's disease. *J Neurosci* **23**, 994-1005.
- [25] Thompson PM, Mega MS, Woods RP, Zoumalan CI, Lindshield CJ, Blanton RE, Moussai J, Holmes CJ, Cummings JL, Toga AW (2001) Cortical change in Alzheimer's disease detected with a disease-specific population-based brain atlas. *Cereb Cortex* **11**, 1-16.
- [26] Thompson PM, Moussai J, Zohoori S, Goldkorn A, Khan AA, Mega MS, Small GW, Cummings JL, Toga AW (1998) Cortical variability and asymmetry in normal aging and Alzheimer's disease. *Cereb Cortex* **8**, 492-509.
- [27] Shi F, Liu B, Zhou Y, Yu C, Jiang T (2009) Hippocampal volume and asymmetry in mild cognitive impairment and Alzheimer's disease: meta-analyses of MRI studies. *Hippocampus* **19**, 1055-1064.
- [28] Janota I, Mountjoy CQ (1988) Asymmetry of pathology in Alzheimer's disease. *J Neurol Neurosurg Psychiatry* **51**, 1011-1012.
- [29] Wilcock GK, Esiri MM (1987) Asymmetry of pathology in Alzheimer's disease. *J Neurol Neurosurg Psychiatry* **50**, 1384-1386.
- [30] Moosy J, Zubenko GS, Martinez AJ, Rao GR, Kopp U, Hanin I (1989) Lateralization of brain morphologic and cholinergic abnormalities in Alzheimer's disease. *Arch Neurol* **46**, 639-642.
- [31] Raji CA, Becker JT, Tsopelas ND, Price JC, Mathis CA, Saxton JA, Lopresti BJ, Hoge JA, Ziolk SK, DeKosky ST, Klunk WE (2008) Characterizing regional correlation, laterality and symmetry of amyloid deposition in mild cognitive impairment and Alzheimer's disease with Pittsburgh Compound B. *J Neurosci Methods* **172**, 277-282.
- [32] Tsai KJ, Yang CH, Lee PC, Wang WT, Chiu MJ, Shen CK (2009) Asymmetric expression patterns of brain transthyretin in normal mice and a transgenic mouse model of Alzheimer's disease. *Neuroscience* **159**, 638-646.
- [33] Gauthier S, Reisberg B, Zaudig M, Petersen RC, Ritchie K, Broich K, Belleville S, Brodaty H, Bennett D, Chertkow H, Cummings JL, de Leon M, Feldman H, Ganguli M, Hampel H, Scheltens P, Tierney MC, Whitehouse P, Winblad B (2006) Mild cognitive impairment. *Lancet* **367**, 1262-1270.
- [34] Petersen RC, Smith GE, Waring SC, Ivnik RJ, Tangalos EG, Kokmen E (1999) Mild cognitive impairment: clinical characterization and outcome. *Arch Neurol* **56**, 303-308.
- [35] Petersen RC, Negash S (2008) Mild cognitive impairment: an overview. *CNS Spectr* **13**, 45-53.
- [36] McKhann G, Drachman D, Folstein M, Katzman R, Price D, Stadlan EM (1984) Clinical diagnosis of Alzheimer's disease: report of the NINCDS-ADRDA Work Group under the auspices of Department of Health and Human Services Task Force on Alzheimer's Disease. *Neurology* **34**, 939-944.
- [37] Bozzali M, Filippi M, Magnani G, Cercignani M, Franceschi M, Schiatti E, Castiglioni S, Mossini R, Falautano M, Scotti G, Comi G, Falini A (2006) The contribution of voxel-based morphometry in staging patients with mild cognitive impairment. *Neurology* **67**, 453-460.
- [38] Ashburner J, Friston KJ (2005) Unified segmentation. *Neuroimage* **26**, 839-851.
- [39] Tohka J, Zijdenbos A, Evans A (2004) Fast and robust parameter estimation for statistical partial volume models in brain MRI. *Neuroimage* **23**, 84-97.
- [40] Rajapakse JC, Giedd JN, Rapoport JL (1997) Statistical approach to segmentation of single-channel cerebral MR images. *IEEE Trans Med Imaging* **16**, 176-186.
- [41] Cuadra MB, Cammoun L, Butz T, Cuisenaire O, Thiran JP (2005) Comparison and validation of tissue modelization and

- statistical classification methods in T1-weighted MR brain images. *IEEE Trans Med Imaging* **24**, 1548-1565.
- [42] Lüders E, Gaser C, Narr KL, Toga AW (2009) Why sex matters: brain size independent differences in gray matter distributions between men and women. *J Neurosci* **29**, 14265-14270.
- [43] Lüders E, Gaser C, Jancke L, Schlaug G (2004) A voxel-based approach to gray matter asymmetries. *Neuroimage* **22**, 656-664.
- [44] Maldjian JA, Laurienti PJ, Kraft RA, Burdette JH (2003) An automated method for neuroanatomic and cytoarchitectonic atlas-based interrogation of fMRI data sets. *Neuroimage* **19**, 1233-1239.
- [45] Smith SM, Nichols TE (2009) Threshold-free cluster enhancement: addressing problems of smoothing, threshold dependence and localisation in cluster inference. *Neuroimage* **44**, 83-98.
- [46] Mitchell J, Arnold R, Dawson K, Nestor PJ, Hodges JR (2009) Outcome in subgroups of mild cognitive impairment (MCI) is highly predictable using a simple algorithm. *J Neurol* **256**, 1500-1509.
- [47] Chetelat G, Desgranges B, De La Sayette V, Viader F, Eustache F, Baron JC (2002) Mapping gray matter loss with voxel-based morphometry in mild cognitive impairment. *Neuroreport* **13**, 1939-1943.
- [48] Chetelat G, Landeau B, Eustache F, Mezenge F, Viader F, de la Sayette V, Desgranges B, Baron JC (2005) Using voxel-based morphometry to map the structural changes associated with rapid conversion in MCI: a longitudinal MRI study. *Neuroimage* **27**, 934-946.
- [49] Karas G, Sluimer J, Goekoop R, van der Flier W, Rombouts SA, Vrenken H, Scheltens P, Fox N, Barkhof F (2008) Amnesic mild cognitive impairment: structural MR imaging findings predictive of conversion to Alzheimer disease. *AJNR Am J Neuroradiol* **29**, 944-949.
- [50] Karas GB, Burton EJ, Rombouts SA, van Schijndel RA, O'Brien JT, Scheltens P, McKeith IG, Williams D, Ballard C, Barkhof F (2003) A comprehensive study of gray matter loss in patients with Alzheimer's disease using optimized voxel-based morphometry. *Neuroimage* **18**, 895-907.
- [51] Karas GB, Scheltens P, Rombouts SA, Visser PJ, van Schijndel RA, Fox NC, Barkhof F (2004) Global and local gray matter loss in mild cognitive impairment and Alzheimer's disease. *Neuroimage* **23**, 708-716.
- [52] Pennanen C, Testa C, Laakso MP, Hallikainen M, Helkala EL, Hanninen T, Kivipelto M, Kononen M, Nissinen A, Tervo S, Vanhanen M, Vanninen R, Frisoni GB, Soininen H (2005) A voxel based morphometry study on mild cognitive impairment. *J Neurol Neurosurg Psychiatry* **76**, 11-14.
- [53] Ullman MT (2001) A neurocognitive perspective on language: the declarative/procedural model. *Nat Rev Neurosci* **2**, 717-726.
- [54] Hickok G, Poeppel D (2000) Towards a functional neuroanatomy of speech perception. *Trends Cogn Sci* **4**, 131-138.
- [55] Leff AP, Schofield TM, Crinion JT, Seghier ML, Grogan A, Green DW, Price CJ (2009) The left superior temporal gyrus is a shared substrate for auditory short-term memory and speech comprehension: evidence from 210 patients with stroke. *Brain* **132**, 3401-3410.
- [56] Apostolova LG, Lu P, Rogers S, Dutton RA, Hayashi KM, Toga AW, Cummings JL, Thompson PM (2008) 3D mapping of language networks in clinical and pre-clinical Alzheimer's disease. *Brain Lang* **104**, 33-41.
- [57] Teipel SJ, Willoch F, Ishii K, Burger K, Drzezga A, Engel R, Bartenstein P, Moller HJ, Schwaiger M, Hampel H (2006) Resting state glucose utilization and the CERAD cognitive battery in patients with Alzheimer's disease. *Neurobiol Aging* **27**, 681-690.